

A Systematic Comparison of Training Objectives for Out-of-Distribution Detection in Image Classification

Furkan Genç
Bilkent University

furkan.genc@bilkent.edu.tr

Onat Özdemir
Middle East Technical University

onat.ozdemir@metu.edu.tr

Emre Akbaş
Middle East Technical University

Abstract

Out-of-distribution (OOD) detection is critical in safety-sensitive applications. While this challenge has been addressed from various perspectives, the influence of training objectives on OOD behavior remains comparatively under-explored. In this paper, we present a systematic comparison of four widely used training objectives: Cross-Entropy Loss, Prototype Loss, Triplet Loss, and Average Precision (AP) Loss, spanning probabilistic, prototype-based, metric-learning, and ranking-based supervision, for OOD detection in image classification under standardized OpenOOD protocols. Across CIFAR-10/100 and ImageNet-200, we find that Cross-Entropy Loss, Prototype Loss, and AP Loss achieve comparable in-distribution accuracy, while Cross-Entropy Loss provides the most consistent near- and far-OOD performance overall; the other objectives can be competitive in specific settings.

1. Introduction

Machine learning models have achieved remarkable success in various domains, such as computer vision, natural language processing, and speech recognition. However, when deployed in real-world applications, these models often encounter data that differs significantly from the training data. It is crucial that these models detect inputs that are out of their training data distribution. This problem, involving inputs outside the distribution of the training data, is known as **out-of-distribution (OOD)** detection. Handling OOD data poses a critical challenge for the reliability and safety of machine learning systems. OOD inputs can lead to unpredictable model behavior, which is unacceptable in safety-critical applications such as autonomous driving, medical diagnosis, and security systems. Therefore, it is of great importance to develop models that can effectively detect and manage OOD data.

Despite significant progress in OOD detection, most existing approaches focus on enhancing post-processing techniques [9, 16, 18, 19, 42] or designing specialized model architectures and training methods [10, 11]. A few studies have examined how representation learning objectives, such as contrastive learning or masked image modeling, affect OOD detection, but systematic comparisons across common supervised objectives remain limited [17, 32, 33, 42]. Training objectives play a crucial role in shaping the feature representations learned by neural networks, directly affecting their ability to distinguish between in-distribution (ID) and OOD samples.

This paper systematically investigates the impact of different training objectives on OOD detection performance in image classification tasks. We take Cross-Entropy Loss [7] as the standard and most widely used classification objective, and compare it against three commonly used alternatives: Triplet Loss [30], Prototype Loss [31], and Average Precision (AP) Loss [3, 27]. These objectives have been successful in settings such as metric learning, few-shot learning, and ranking-based training [2, 3, 12, 30, 31]. However, their relative behavior for OOD detection is less systematically characterized, and most objective-focused OOD studies either analyze representation or pretraining objectives or propose OOD-specific losses rather than comparing common supervised objectives head-to-head [17, 22, 25, 32, 42].

Triplet Loss, introduced in FaceNet [30], compares an anchor input to a positive input (same class) and a negative input (different class). By minimizing the distance between the anchor and the positive and maximizing the distance to the negative, the model learns to recognize similarities and differences in the embedding space. Prototype Loss, proposed by Snell et al. [31], represents each class by a prototype embedding and trains the model to minimize the distance between a sample’s embedding and its corresponding class prototype, while maximizing separation from the

prototypes of other classes. Average Precision (AP) Loss [3, 27] is a ranking-based objective that optimizes the ordering of scores by promoting higher scores for positive (in-class) examples than for negatives, aiming to improve separability in terms of score rankings.

While these training objectives have been successfully applied in other domains, their effectiveness for OOD detection has not been thoroughly studied. Most OOD detection baselines start from a classifier trained with Cross-Entropy Loss and study post-hoc confidence scoring for detection [9, 16, 18, 19], with limited exploration of alternative training objectives in the OOD detection context. Additionally, using benchmarks such as **OpenOOD** [41] has standardized evaluation protocols for OOD detection, facilitating fair comparisons between methods. OpenOOD v1.5 [43] extends the capabilities of the original benchmark by incorporating a broader range of OOD datasets and supporting multiple detection tasks, including detection under covariate shift and semantic shift. However, the influence of training objectives within these benchmarks remains under-explored.

By evaluating these training objectives on standard image classification datasets using the OpenOOD benchmark, we aim to provide a comprehensive understanding of their impact on ID accuracy and OOD detection performance.

We select Cross-Entropy, Triplet, Prototype, and AP losses as representative instances of four widely used supervised paradigms: probabilistic classification, metric learning, prototype-based learning, and ranking-based optimization, each with a standard inference rule for classification and confidence scoring. This selection enables a controlled, objective-level comparison under a fixed backbone and standardized OpenOOD protocols, while minimizing auxiliary design degrees of freedom. Objectives that require additional components (e.g., specialized augmentation pipelines, large-batch sampling machinery, or extra regularization terms) are intentionally left outside our scope, as they would introduce confounders beyond the training objective itself.

The main contributions of this paper are:

- We provide a systematic comparison of four widely used training objectives: Cross-Entropy, Triplet, Prototype, and Average Precision losses, covering probabilistic, metric-learning, prototype-based, and ranking-based supervision paradigms for image classification.
- We use the OpenOOD benchmark [43] with a fixed backbone and standardized protocols to isolate the effect of the training objective and enable fair, reproducible evaluation.
- We analyze the trade-offs induced by each objective on in-distribution accuracy and near-/far-OOO detection, offering practical guidance on when each loss family is a reasonable default.

Our findings suggest that specialized training objectives, such as Triplet Loss and Prototype Loss, can offer certain benefits, yet Cross-Entropy Loss remains a strong baseline for ID accuracy and OOD detection. This study provides valuable guidance for researchers and practitioners in selecting appropriate training objectives for OOD detection tasks.

2. Related Work

Out-of-distribution (OOD) detection is a critical area of machine learning research, focusing on models' ability to recognize and appropriately handle inputs that differ significantly from the training data. This section reviews key studies on OOD detection, emphasizing training objectives, evaluation benchmarks like OpenOOD, and methodologies relevant to our work.

2.1. Out-of-Distribution Detection Methods

Early work [9] introduced the concept of using the *maximum softmax probability* from a classifier as a baseline for OOD detection. This simple yet effective approach highlighted the potential of leveraging existing classifiers for OOD tasks.

Building on this, ODIN [18] improved OOD detection by applying temperature scaling and input perturbations to enhance the discriminative power of softmax scores. Lee et al. [16] introduced a method using Mahalanobis distance-based confidence scores computed from layer activations, achieving significant improvements in OOD detection performance.

Beyond softmax- and Mahalanobis-based confidence scores, energy-based scoring has become a widely used alternative for OOD detection [19]. More recently, GEN [20] revisits and strengthens softmax-based OOD detection with improved calibration and post-hoc scoring. In parallel, non-parametric nearest-neighbor distances in deep feature space have been shown to be effective OOD scores, especially when the feature distribution violates simple parametric assumptions [32].

Complementary to these post-hoc scoring functions, training-time strategies such as Outlier Exposure [10] incorporate additional outlier data to improve OOD detection, while AugMix [11] improves robustness through augmentation and can strengthen uncertainty estimates.

2.2. Training Objectives

Cross-Entropy Loss remains the standard loss function for classification tasks due to its effectiveness in optimizing probabilistic models [7]. However, it does not explicitly enforce intra-class compactness and large inter-class separation in the feature space, which may limit its effectiveness in OOD detection when the ID and OOD classes are not well separated.

Metric Learning Losses, such as Contrastive Loss and Triplet Loss, have been explored to learn embeddings where similar instances are closer and dissimilar ones are farther apart [4, 30]. While Triplet Loss has succeeded in face recognition and person re-identification [12], its application to OOD detection is less common.

Prototypical Networks [31] and related prototype-based methods have been widely used in few-shot learning [29, 45]. Learning a prototype for each class can generalize these methods to new classes with limited samples.

Average Precision Loss [3, 27], which directly optimizes ranking metrics such as the average precision, has been used in information retrieval and imbalanced classification tasks [2]. Although Average Precision Loss can be adapted for OOD detection to improve ID-OOD ranking, it remains less commonly adopted than standard classification-based objectives.

Beyond comparing common supervised objectives, prior work has investigated how the training or pre-training objective influences OOD behavior. Sun et al. [32] study nearest-neighbor OOD detection and report differences between representations learned with contrastive-style objectives versus standard CE training. Li et al. [17] analyze how masked image modeling pre-training affects OOD detection performance. Other works propose objectives explicitly designed to improve OOD detection by shaping the embedding geometry, such as hyperspherical embeddings [25] or mixtures of prototypes [22]. Our work complements these efforts by providing a systematic comparison of four widely used supervised objectives under a fixed architecture and standardized OpenOOD evaluation, clarifying the trade-offs of common objective families before introducing OOD-specific training objectives.

2.3. OpenOOD Benchmark

The evaluation of OOD detection methods has been significantly advanced by introducing standardized benchmarks, such as OpenOOD [41]. Building on this foundation, OpenOOD v1.5 [43] provides a more comprehensive framework with additional datasets, enhanced evaluation protocols, and improved metrics for OOD detection, enabling fairer and more robust comparisons across methods.

OpenOOD offers a collection of datasets categorized into **near-OOD** and **far-OOD** based on their similarity to the in-distribution data, where near-OOD samples are semantically or visually closer to the ID classes, while far-OOD samples differ more substantially from the ID distribution. This allows researchers to evaluate models under varying degrees of distributional shift. Despite its importance, the impact of the loss function on performance under this benchmark has not been thoroughly studied. Our work leverages OpenOOD to systematically evaluate how different loss functions affect OOD detection performance,

thereby filling a gap in the literature.

3. Methodology

This section describes our methodology, encompassing the model architectures, training objectives, out-of-distribution (OOD) detection strategies, and inference procedures.

3.1. Model Architecture

We employ ResNet-18 [8] using the default OpenOOD implementations [43]. For objectives that operate on class logits (Cross-Entropy and AP), we set the final fully connected (FC) layer to output C logits, where C is the number of in-distribution classes. For embedding-based objectives (Triplet and Prototype), we replace the final FC layer with an embedding head of dimension ED and treat its output as $f(x)$ for metric/prototype inference. For CIFAR-10/100, the initial layers are modified to accommodate 32×32 images, whereas for ImageNet-200, we use the standard ResNet-18 architecture.

3.2. Training Objectives and Inference

In our experiments, we compare four training objectives: Cross-Entropy Loss [7], Triplet Loss [30], Prototype Loss [31], and Average Precision (AP) Loss [3, 27]. The selected hyperparameters and the OOD post-processing rule used for each dataset-objective pair are summarized in Appendix A (Tables 1-3).

We chose these objectives to represent common supervision paradigms: probabilistic alignment (Cross-Entropy), margin-based metric learning (Triplet), prototype-based clustering (Prototype), and ranking-based supervision (AP). Cross-Entropy trains a classifier by maximizing the likelihood of the ground-truth class under a softmax distribution over logits. Prototype-based training replaces logits with distances to learned class prototypes, encouraging intra-class compactness around each prototype. Triplet training learns an embedding space by enforcing a margin between the distances from the positive to the anchor and from the negative to the anchor. Finally, AP training uses ranking-based supervision to promote higher scores for positives than negatives, aiming to improve ordering quality.

We define all OOD scores so that higher values indicate greater OOD likelihood. Because these objectives produce different natural outputs (e.g., logits vs. embeddings), we evaluate each model using OOD scoring rule(s) that are standard and naturally aligned with the corresponding objective family. For Cross-Entropy and Prototype training, we consider MSP-based scoring (i.e., $-\max_c p_c(x)$) and predictive-entropy scoring and report the selected rule for each dataset-objective pair (Appendix A). For Triplet training, we use the standard nearest-neighbor distance in the learned embedding space (i.e., the minimum distance to the

training embeddings). For AP training, we treat the per-class scores $s_c(x)$ as logits, compute class probabilities via softmax, and use predictive entropy (Eq. 4).

Accordingly, our comparison is intentionally scoped to *objective-inference pairings* that are standard in practice, including probability-based scoring (such as MSP/entropy for CE/Prototype/AP) and distance-to-training-embeddings for Triplet. This design mirrors real deployment, where the training objective dictates the natural form of confidence used for OOD scoring. While using a single universal detector for all objectives could further isolate the objective effect, doing so would require introducing additional modeling assumptions (e.g., converting embeddings to calibrated class probabilities or fitting extra density models), which would confound the study with extra design choices beyond the loss itself.

3.2.1. Cross-Entropy Loss

Cross-Entropy Loss is a widely used loss function for multi-class classification tasks. It measures the discrepancy between the predicted probability distribution and the actual distribution. The loss for a single sample is defined as:

$$L_{\text{CE}} = - \sum_{c=1}^C y_c \log(p_c) \quad (1)$$

where C is the number of classes, y is the ground truth label encoded as a one-hot vector, and y_c is its c^{th} element, i.e. we have $y = [y_1, y_2, \dots, y_C]$. p_c is the predicted probability for class c , obtained by applying the softmax function to the network’s output logits.

During inference, the class with the highest probability is selected as the predicted label:

$$\hat{y}(x) = \arg \max_c p_c(x) \quad (2)$$

We test two OOD scoring methods: (i) Maximum Softmax Probability (MSP) [9]:

$$S_{\text{OOD}}(x) = - \max_c p_c(x) \quad (3)$$

and (ii) Entropy of Softmax Probabilities:

$$S_{\text{OOD}}(x) = - \sum_{c=1}^C p_c(x) \log p_c(x). \quad (4)$$

3.2.2. Triplet Loss

Triplet Loss [30] is a metric learning loss function designed to learn an embedding space where samples of the same class are closer together and samples of different classes are farther apart. The loss for a triplet of samples (anchor a , positive p , negative n) is defined as:

$$L_{\text{Triplet}} = \max(0, D(f(a), f(p)) - D(f(a), f(n)) + \alpha) \quad (5)$$

where $f(\cdot)$ is the learned embedding function, $D(u, v)$ is the squared Euclidean distance, and α is the margin hyperparameter ensuring minimum class separation in the embedding space. In all triplet-loss experiments, we use a fixed margin of $\alpha = 1$.

In the Triplet Loss framework [30], we select a triplet (x_a, x_p, x_n) such that

$$\|f(x_a) - f(x_p)\|_2^2 + \alpha < \|f(x_a) - f(x_n)\|_2^2. \quad (6)$$

We utilize a Random Negative Triplet Selector for CIFAR-10 [13], which employs random triplet sampling. However, for CIFAR-100 [13] and ImageNet-200 [5, 35], we employ a Semi-Hard Negative Triplet Selector. In this approach, negatives are chosen so that they are farther from the anchor than the positive sample, but still within the margin. Let $d_{ap} = \|f(x_a) - f(x_p)\|_2^2$ and $d_{an} = \|f(x_a) - f(x_n)\|_2^2$. Semi-hard negatives satisfy

$$d_{ap} < d_{an} < d_{ap} + \alpha. \quad (7)$$

The choice between Random and Semi-Hard selectors across datasets was based on validation performance, ensuring each dataset used a stable, effective mining strategy that matched its class complexity. Intuitively, CIFAR-10’s lower class count makes random mining sufficiently informative and often more stable, while semi-hard mining becomes beneficial as class diversity increases (CIFAR-100/ImageNet-200), where naive sampling more frequently yields uninformative negatives.

The predicted class is determined by identifying the nearest training embedding:

$$\hat{y}(x) = y \left(\arg \min_{x_i^{\text{train}}} D(f(x), f(x_i^{\text{train}})) \right), \quad (8)$$

where $y(\cdot)$ returns the ground-truth label of the example. OOD Score is computed as the minimum distance to the training embeddings:

$$S_{\text{OOD}}(x) = \min_i D(f(x), f(x_i^{\text{train}})). \quad (9)$$

This distance-to-training-set score is closely related to deep nearest-neighbor OOD detection methods [32].

3.2.3. Prototype Loss

For the prototype learning approach, we employ the *Generalized Convolutional Prototype Learning (GCPL)* method [40]. The prototype loss in GCPL has two components with a balancing hyperparameter λ :

$$L_{\text{Total}} = L_{\text{DCE}} + \lambda L_{\text{Center}}, \quad (10)$$

where L_{DCE} is the distance-based cross-entropy loss, and L_{Center} is the center loss promoting intra-class compactness.

L_{DCE} is defined as

$$L_{\text{DCE}} = - \sum_{i=1}^N \log \frac{\exp(-\tau D(f(x_i), m_{y_i}))}{\sum_{k=1}^C \exp(-\tau D(f(x_i), m_k))} \quad (11)$$

where $f(x_i)$ is the embedding of example x_i , m_k is the prototype (mean embedding) of class k , $D(\cdot, \cdot)$ is the squared Euclidean distance. τ is a temperature hyperparameter controlling the sharpness of the probability distribution. For each dataset-objective pair, τ is selected based on validation performance and reported in Appendix A. And, L_{Center} is defined as follows:

$$L_{\text{Center}} = \frac{1}{N} \sum_{i=1}^N \|f(x_i) - m_{y_i}\|_2^2. \quad (12)$$

The predicted class is determined by the nearest class prototype:

$$\hat{y}(x) = \arg \min_c D(f(x), m_c) \quad (13)$$

We test two OOD scoring methods as in the Cross-Entropy setting: (i) MSP as in Equation (3) and (ii) entropy as in Equation (4). In both cases, the class probability $p_c(x)$ is computed using the selected temperature parameter τ :

$$p_c(x) = \frac{\exp(-\tau D(f(x), m_c))}{\sum_{k=1}^C \exp(-\tau D(f(x), m_k))}. \quad (14)$$

3.2.4. Average Precision (AP) Loss

The Average Precision Loss [3, 27] is a ranking-based loss, which is designed to directly optimize the Average Precision (AP) evaluation measure. For binary classification, the AP Loss is defined as 1 minus average precision:

$$L_{\text{AP}} = 1 - \frac{1}{|P|} \sum_{i \in P} \text{prec}(i), \quad (15)$$

where $\text{prec}(i)$ is the precision of the i^{th} positive example. This can be expressed as the ratio of the rank of the i^{th} positive example among all positives and the rank of the same example among all examples (negatives included):

$$\text{prec}(i) = \frac{\text{rank}_{\text{pos}}(i)}{\text{rank}(i)}. \quad (16)$$

The $\text{rank}(\cdot)$ operator induces discrete ordering via pairwise comparisons and is not differentiable in its exact form. Following [27], we implement AP-style optimization using the standard three-step ranking-loss formulation over score differences and incorporate the paper’s identity/error-driven update for the non-differentiable primary-term step within backpropagation, which provides well-defined gradients with respect to logits and enables end-to-end optimization with SGD.

We adopt a one-vs-all approach for each class c to extend the AP Loss to multi-class classification. For each class, we

treat samples belonging to class c as positives ($y_i = 1$) and all other samples as negatives ($y_i = 0$). We compute the AP Loss for each class and then sum over all classes:

$$L_{\text{Total}} = \sum_{c=1}^C L_{\text{AP}}^{(c)} \quad (17)$$

For other details, the reader is referred to [3, 27]. The predicted class is the arg-max of $p_c(x)$ where

$$p_c(x) = \frac{\exp(s_c(x))}{\sum_{k=1}^C \exp(s_k(x))}. \quad (18)$$

OOD score is the same as Equation (4).

4. Experiments

In this section, we evaluate four training objectives: Cross-Entropy Loss, Triplet Loss, Prototype Loss, and Average Precision (AP) Loss on standard image classification datasets for Out-of-Distribution (OOD) detection.

Datasets. We train models on three datasets: CIFAR-10 [13], CIFAR-100 [13] and ImageNet-200 [5, 35]. For these three datasets, which are also referred to as the ID (in-distribution) dataset, the OpenOOD benchmark defines the following near- and far-OOD datasets: For **CIFAR-10**, near-OOD: CIFAR-100, TinyImageNet [15]; far-OOD: MNIST [6], SVHN [26], Texture [14], Places365 [44]. For **CIFAR-100**, near-OOD: CIFAR-10, TinyImageNet; far-OOD: MNIST, SVHN, Texture, Places365. For **ImageNet-200** [5], near-OOD: SSB-hard [37], NINCO [1]; far-OOD: iNaturalist [36], Texture, OpenImage-O [38].

Evaluation Metrics. To evaluate models, we use the following metrics from the OpenOOD benchmark: In-Distribution (ID) accuracy is the classification accuracy on the test set of the ID dataset. Area Under the Receiver Operating Characteristic Curve (AUROC) measures the model’s ability to distinguish between ID and OOD samples across all classification thresholds. We report both near-OOD AUROC and far-OOD AUROC. A higher AUROC indicates better discrimination between ID and OOD samples.

Implementation Details. All experiments are implemented using PyTorch [28]. We utilize the OpenOOD framework [43] for standardized dataset loading and evaluation. For transparency and reproducibility, we report the chosen learning rate, embedding dimension (when applicable), Prototype parameters (λ, τ), the Triplet mining strategy (Random vs. Semi-Hard), and the selected OOD scoring rule for each setting in Appendix A.

Training Configuration. We use stochastic gradient descent (SGD) as an optimizer with a momentum of 0.9 and a weight decay of 5×10^{-4} . We set the batch size to 128 for CIFAR-10 and CIFAR-100, and 256 for ImageNet-200. We use a cosine annealing learning rate schedule without warm restarts [21], with an initial learning rate chosen for each loss function. We train the models for 100 epochs on CIFAR-10 and CIFAR-100, and for 90 epochs on ImageNet-200, following the default OpenOOD training schedule for this benchmark to keep our setup aligned with the standard evaluation protocol. For each loss function, we perform hyperparameter tuning over a range of learning rates and other loss-specific parameters.

5. Results

We run five independent experiments for each training objective on every dataset to ensure robust estimates. We present our quantitative findings using bar charts sorted from highest to lowest performance for each metric. In these graphs, adjacent methods in the sorted order are compared using Welch’s t -tests ($p < 0.05$) over the five-run distributions. The pairs that differ significantly are marked with (**).

We use Welch’s t -test rather than Student’s t -test since it does not assume equal variances and is appropriate for comparing mean performance across independent training runs where variability can differ across objectives [39]. We do not apply McNemar’s test [24] as it is designed for paired comparisons of discrete decisions on the same examples at a fixed operating point, whereas our primary metrics are computed from continuous confidence scores (notably AUROC) and are summarized at the run level.

We show three plots per dataset: (a) ID Accuracy, (b) near-OOD AUROC, and (c) far-OOD AUROC. The abbreviations in the figures are as follows: AP denotes AP Loss, CE stands for Cross-Entropy Loss, PT represents Prototype Loss, and TL indicates Triplet Loss. Unless otherwise stated, we report results using the selected post-processing rule for each dataset-objective pair listed in Appendix A. Complete numeric results are provided in Appendix B.

5.1. CIFAR-10 Results

As shown in Figure 1, on CIFAR-10, Prototype Loss and Cross-Entropy Loss achieve the best ID accuracy of 95.06% and 94.95%, respectively, with no statistically significant difference between them. AP Loss and Triplet Loss provide the strongest OOD detection overall: Triplet Loss achieves the best near-OOD AUROC (88.85%), while AP Loss achieves the best far-OOD AUROC (92.34%), with each being second-best on the other OOD setting (AP: 88.80% near; Triplet: 92.25% far). While Triplet Loss maintains competitive OOD detection performance (88.85% near, 92.25% far), it performs the worst in ID accuracy (93.56%).

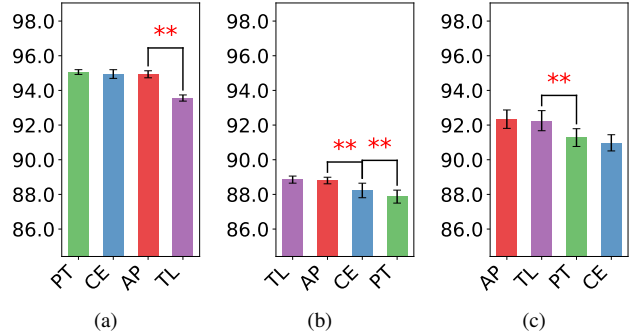


Figure 1. Performance metrics for **CIFAR-10** on the OpenOOD benchmark: (a) ID Accuracy, (b) near-OOD AUROC, and (c) far-OOD AUROC. ** denotes statistically significant difference. AP: AP Loss, CE: Cross-Entropy Loss, PT: Prototype Loss, TL: Triplet Loss.

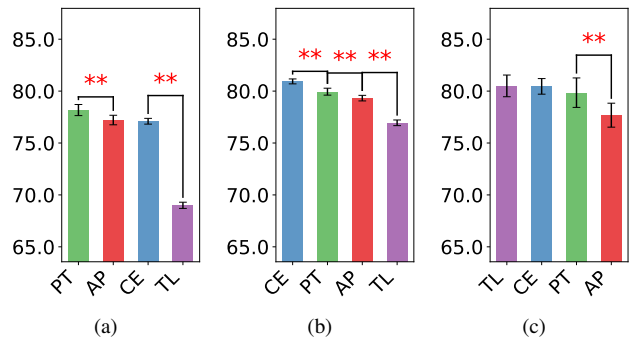


Figure 2. Performance metrics for **CIFAR-100** on the OpenOOD benchmark: (a) ID Accuracy, (b) near-OOD AUROC, and (c) far-OOD AUROC. ** denotes statistically significant difference. AP: AP Loss, CE: Cross-Entropy Loss, PT: Prototype Loss, TL: Triplet Loss.

Overall, none of the training objectives consistently dominates across all three metrics.

5.2. CIFAR-100 Results

Referring to Figure 2, we observe that on CIFAR-100, the Cross-Entropy Loss model achieves the best near-OOD AUROC (80.94%) and competitive far-OOD AUROC (80.46%), yielding the strongest overall balance among objectives as class count increases. The Prototype Loss model achieves the highest ID classification accuracy (78.18%), indicating effective intra-class compactness and discriminative feature learning. The AP Loss model shows moderate near-OOD detection at 79.32%, performs worse for far-OOD detection at 77.68%, and slightly lags behind Prototype Loss in ID accuracy at 77.21%. Meanwhile, the Triplet Loss model attains the best far-OOD AUROC (80.50%) but at the cost of substantially lower ID accuracy (69.00%) and weaker near-OOD detection (76.95%), suggesting that met-

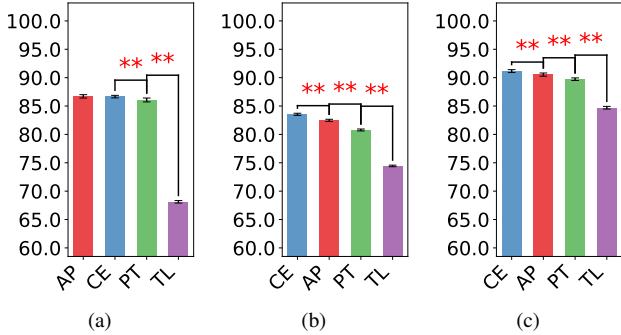


Figure 3. Performance metrics for **ImageNet-200** on the OpenOOD benchmark: (a) ID Accuracy, (b) near-OOD AUROC, and (c) far-OOD AUROC. ** denotes statistically significant difference. AP: AP Loss, CE: Cross-Entropy Loss, PT: Prototype Loss, TL: Triplet Loss.

ric learning can improve separation for some far-OOD shifts while scaling poorly in class-diverse regimes.

5.3. ImageNet-200 Results

Figure 3 illustrates the performance on ImageNet-200, where the Cross-Entropy Loss model demonstrates the most robust performance in OOD detection (83.54% near, 91.16% far) and nearly matches AP Loss in ID accuracy (86.66% vs. 86.71%), suggesting its scalability and reliability under more complex, large-scale conditions. Although the AP Loss (86.71%) and Prototype Loss (86.07%) models remain strong contenders in ID Accuracy, neither surpasses the effectiveness of Cross-Entropy Loss in OOD detection. This outcome suggests that while metric learning approaches are beneficial, they may not provide a clear advantage at larger dataset scales. Meanwhile, the Triplet Loss model continues to struggle, with ID accuracy at 68.12% and OOD detection at 74.44% (near) and 84.70% (far). This may be due to the increased difficulty of forming informative triplets within an expansive, diverse class set, leading to comparatively weaker embeddings.

5.4. Qualitative Analysis

In this section, we provide t-SNE [34] visualizations of embeddings for ID versus near- and far-OOD comparisons generated by models trained with different loss functions. Appendix C provides extended qualitative analysis, including UMAP [23] embeddings for ID versus OOD, and ID versus near- and far-OOD comparisons. Both t-SNE and UMAP methods are widely recognized for their effectiveness in visualizing high-dimensional data, but they employ different underlying principles and have distinct advantages. t-SNE is particularly adept at revealing local structures but may distort global relationships, whereas UMAP provides a more balanced view of both local and global

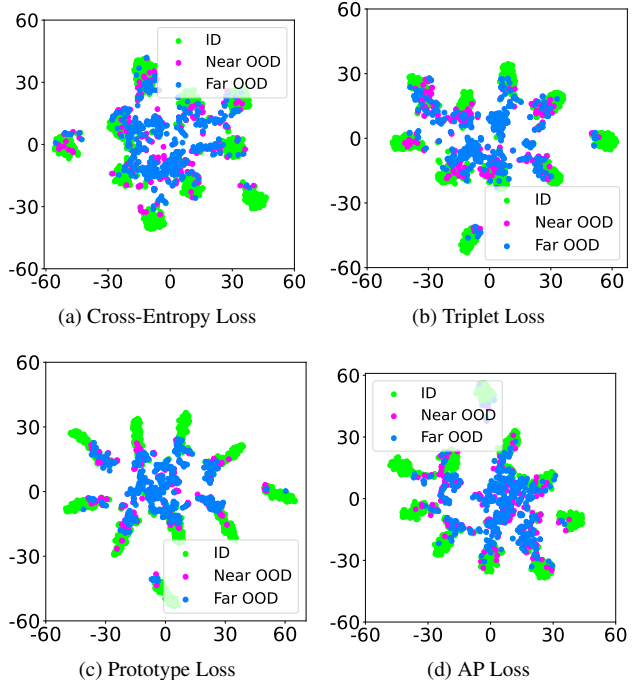


Figure 4. t-SNE visualizations for ID vs near-OOD and far-OOD samples.

structures while improving computational efficiency. Because t-SNE and UMAP do not preserve exact pairwise distances from the original feature space, we use them only for qualitative analysis, aiming to compare how different training objectives shape the clustering and separation of in-distribution (ID) and out-of-distribution (OOD) samples. Visual patterns, such as tighter ID clustering or better OOD separation, can reveal valuable insights into the discriminative capacity and generalization behavior of learned embeddings, thus supporting and enriching our quantitative results.

For better observability, the CIFAR-10 dataset with fewer classes is used. The images in the following datasets are used as near-OOD and far-OOD samples in the visualizations:

- **Near-OOD:** CIFAR-100, TinyImageNet.
- **Far-OOD:** MNIST, SVHN, Textures, Places365.

As out-of-distribution samples become more similar to the training data, separating ID and OOD instances becomes more challenging. Hence, it is important to analyze the performance of the methods in these two cases separately.

Figure 4 shows the visualizations of the data points belonging to in-distribution (ID), near out-of-distribution (near-OOD), and far out-of-distribution (far-OOD) samples. Far-OOD instances tend to appear in regions of the projection that are visually separated from the dense ID class clus-

ters and not strongly aligned with any single cluster. This qualitative pattern is consistent with the nature of far-OOD data, whose classes often exhibit visual features that differ substantially from the ID classes. As a result, far-OOD points often appear in regions that are not clearly aligned with any single ID class cluster. This observation is consistent with the intuition behind the OOD scoring methods we use to detect out-of-distribution samples:

Maximum Softmax Probability (MSP): MSP is higher for locations closer to ID examples. Therefore, MSP values will be low for far-OOD samples, as these samples are not close to any of the ID classes.

Minimum Distance to Prototypes/Train Samples: The distances between the far-OOD samples and the prototypes/samples belonging to the ID classes are higher compared to the ID instances. Hence, a threshold based on the distance between the given sample and the ID prototypes/samples can be used to distinguish the far-OOD samples from the ID ones.

Entropy of Softmax over Distances/Probabilities: Far-OOD samples often do not align strongly with any single ID class, and may exhibit relatively similar distances to multiple classes in the embedding space. For the same reason, we expect the models to produce class predictions with similar probabilities for far-OOD instances. The entropy of a set of values increases as the values become closer to each other. Hence, for a given far-OOD sample, the entropy of both the list of class prediction probabilities and the distances between the sample and the ID prototypes would be high.

The near-OOD instances, on the other hand, tend to appear closer to the ID classes, as, by definition, their visual features are similar to those of the training data. This situation makes it more difficult to distinguish them from ID examples. Some near-OOD instances appear visually close to ID clusters in the projections, making it harder to distinguish them from ID samples. Hence, the methods we use to identify out-of-distribution instances may perform worse at detecting near-OOD samples than far-OOD ones. This hypothesis is also justified by the quantitative results shared in the previous sections, where the far-OOD AUROC scores are typically better than the near-OOD AUROC scores.

Although the qualitative analysis provides helpful insights into the distribution of ID, near-OOD, and far-OOD instances, there is no clear indication that any method would perform better than others on the OOD detection task.

6. Discussion

The experimental results provide several key insights into the effectiveness of different training objectives for OOD

detection across various datasets. Below, we delve deeper into these findings, discussing the strengths and limitations of each training objective and their interactions with OOD detection capabilities.

- **Cross-Entropy Loss:** Cross-Entropy Loss remains a strong baseline for OOD detection across all evaluated datasets. Its probabilistic modeling facilitates the effective handling of multiple classes, especially evident in the larger-scale ImageNet-200 dataset. The consistency of Cross-Entropy Loss in achieving high ID accuracy and robust OOD detection metrics underscores its reliability and scalability.
- **Triplet Loss:** Although conceptually attractive for metric learning, Triplet Loss faces significant challenges in scaling to datasets with many classes, such as CIFAR-100 and ImageNet-200. The complexity of triplet sampling in high-dimensional and highly class-diverse spaces likely contributes to its underperformance in ID accuracy and OOD detection metrics. Additionally, the computational overhead of generating and processing triplets limits its practicality in large-scale applications.
- **Prototype Loss:** Prototype Loss strikes a balance between classification performance and OOD detection. It excels in achieving high ID accuracy, particularly on datasets with moderate class complexity, such as CIFAR-10 and CIFAR-100. Prototype Loss effectively captures intra-class variations by learning class prototypes, thereby facilitating robust classification. However, its OOD detection performance, while competitive, does not surpass Cross-Entropy Loss across all datasets. This suggests that while Prototype Loss enhances classification, additional mechanisms may be necessary to fully leverage its embedding space for OOD detection.
- **Average Precision (AP) Loss:** AP Loss shows strong ID accuracy, particularly in CIFAR-10 and ImageNet-200. By optimizing for average precision, it effectively ranks OOD samples and achieves robust AUROC scores in these datasets. However, on CIFAR-100, it shows slightly lower ID accuracy and noticeably weaker OOD detection, while on ImageNet-200, its OOD detection does not outperform Cross-Entropy Loss.

Relation to prior findings. Our distance-based inference for Triplet training aligns with the motivation of deep nearest-neighbor OOD scoring [32], but our results suggest that triplet-based training can become difficult to scale as class count grows, which can offset the benefits of metric structure. In contrast to works that study pre-training objective effects (e.g., masked image modeling [17]), we keep the backbone and training pipeline fixed to isolate the supervised objective. Finally, compared to OOD-tailored objectives that explicitly reshape embedding geometry (e.g., hyperspherical embeddings [25] and mixtures of proto-

types [22]), our findings provide baseline trade-offs for widely used objective families that such specialized objectives can be compared against under the same OpenOOD protocols.

Impact of Training Objective Design on OOD Detection:

Our study highlights the significant role that training objective design plays in OOD detection performance. While traditional classification losses, such as Cross-Entropy, provide a strong foundation, specialized losses like AP Loss and Prototype Loss can improve specific performance. However, the benefits often come with trade-offs, such as reduced OOD detection performance or increased computational complexity. Selecting the appropriate training objective depends on the application’s requirements, balancing the need for high classification accuracy with robust OOD detection.

Scalability and Computational Considerations: Cross-Entropy Loss and Prototype Loss demonstrate scalability across datasets of varying complexity, maintaining high performance without excessive computational demands. In contrast, Triplet Loss faces scalability issues due to its reliance on triplet sampling, which becomes increasingly challenging as the number of classes grows. AP Loss typically offers robust OOD detection with modest computational overhead, though it may falter on some datasets. The choice of training objective should consider both performance gains and computational resources, especially in real-world applications where efficiency is critical.

Limitations. Our study has several limitations. Hyperparameter tuning was conducted over a modest range due to computational constraints, and all experiments were performed with a single backbone, so stronger configurations or different architectures may alter some of the observed trends. In addition, the training objective and OOD scoring rule are not fully factorized, since each objective is evaluated with the confidence measure most natural to its output space; we adopt this design to avoid introducing extra calibration or density-estimation components, but a fully crossed comparison of objectives, scoring rules, and operating-point metrics remains important future work.

Future Work. Future directions include extending this foundational comparison to additional objective families (e.g., contrastive or self-supervised pretraining objectives), testing whether the observed trends hold under different backbones and stronger post-hoc scoring methods, and studying hybrid objectives that combine probabilistic and metric-based supervision. These extensions would further clarify how the choice of training objective shapes ID performance and OOD behavior across settings.

7. Conclusion

In this study, we presented a systematic comparison of four widely used training objectives: Cross-Entropy Loss, Triplet Loss, Prototype Loss, and Average Precision (AP) Loss as representative instances of four common supervised training paradigms: probabilistic classification (CE), margin-based metric learning (Triplet), prototype-based learning (Prototype), and ranking-based optimization (AP). Under a fixed architecture and standardized OpenOOD evaluation, we observed that Cross-Entropy Loss remains a strong and reliable baseline, while AP Loss can achieve competitive OOD detection without sacrificing in-distribution (ID) accuracy. Prototype Loss tends to favor ID classification performance, whereas Triplet Loss exhibits clear scalability challenges in larger, multi-class regimes.

Overall, our results highlight that the choice of training objective induces consistent trade-offs between ID accuracy and near- and far-OOO detection. Rather than proposing a new detection method, we aim to clarify the empirical behavior of these common objective families and provide practical guidance for selecting a reasonable default under typical OOD evaluation protocols.

References

- [1] Julian Bitterwolf, Maximilian Mueller, and Matthias Hein. In or out? fixing imagenet out-of-distribution detection evaluation. In *International Conf. on Machine Learning*, 2023. 5
- [2] Andrew Brown, Weidi Xie, Vicky Kalogeiton, and Andrew Zisserman. Smooth-ap: Smoothing the path towards large-scale image retrieval. In *European Conference on Computer Vision*, 2020. 1, 3
- [3] Kean Chen, Jianguo Li, Weiyao Lin, John See, Ji Wang, Lingyu Duan, Zhibo Chen, Changwei He, and Junni Zou. Towards accurate one-stage object detection with ap-loss. In *IEEE/CVF Conference on Computer Vision and Pattern Recognition*, 2019. 1, 2, 3, 5
- [4] Sumit Chopra, Raia Hadsell, and Yann LeCun. Learning a similarity metric discriminatively, with application to face verification. In *IEEE/CVF Conference on Computer Vision and Pattern Recognition*, pages 539–546, 2005. 3
- [5] Jia Deng, Wei Dong, Richard Socher, Li-Jia Li, Kai Li, and Li Fei-Fei. Imagenet: A large-scale hierarchical image database. In *IEEE/CVF Conference on Computer Vision and Pattern Recognition*, pages 248–255, 2009. 4, 5
- [6] Li Deng. The mnist database of handwritten digit images for machine learning research. *IEEE Signal Processing Magazine*, 29(6):141–142, 2012. 5
- [7] Ian Goodfellow, Yoshua Bengio, Aaron Courville, and Bengio. *Deep Learning*. MIT Press, 2016. <http://www.deeplearningbook.org>. 1, 2, 3
- [8] Kaiming He, Xiangyu Zhang, Shaoqing Ren, and Jian Sun. Deep residual learning for image recognition. In *IEEE/CVF*

- Conference on Computer Vision and Pattern Recognition*, 2016. 3
- [9] Dan Hendrycks and Kevin Gimpel. A baseline for detecting misclassified and out-of-distribution examples in neural networks. In *International Conf. on Learning Representations*, 2017. 1, 2, 4
- [10] Dan Hendrycks, Mantas Mazeika, and Thomas Dietterich. Deep anomaly detection with outlier exposure. In *International Conf. on Learning Representations*, 2019. 1, 2
- [11] Dan Hendrycks, Norman Mu, Ekin D Cubuk, Barret Zoph, Justin Gilmer, and Balaji Lakshminarayanan. Augmix: A simple data processing method to improve robustness and uncertainty. In *International Conf. on Learning Representations*, 2020. 1, 2
- [12] Alexander Hermans, Lucas Beyer, and Bastian Leibe. In defense of the triplet loss for person re-identification. *arXiv preprint arXiv:1703.07737*, 2017. 1, 3
- [13] Alex Krizhevsky, Geoffrey Hinton, et al. Learning multiple layers of features from tiny images. Technical report, University of Toronto, 2009. 4, 5
- [14] G. Kylberg. The kylberg texture dataset v. 1.0. Technical Report External report (Blue series) No. 35, Centre for Image Analysis, Swedish University of Agricultural Sciences and Uppsala University, 2011. Available online at: <http://www.cb.uu.se/~gustaf/texture/> and <https://kylberg.org/datasets/>. 5
- [15] Yann Le and Xuan Yang. Tiny imagenet visual recognition challenge. Technical report, Stanford University, 2015. Available online at: https://cs231n.stanford.edu/reports/2015/pdfs/yle_project.pdf. 5
- [16] Kimin Lee, Kibok Lee, Honglak Lee, and Jinwoo Shin. A simple unified framework for detecting out-of-distribution samples and adversarial attacks. In *Advances in Neural Information Processing Systems*, 2018. 1, 2
- [17] Jingyao Li, Pengguang Chen, Zexin He, Shaozuo Yu, Shu Liu, and Jiaya Jia. Rethinking out-of-distribution (ood) detection: Masked image modeling is all you need. In *CVPR*, 2023. 1, 3, 8
- [18] Shiyu Liang, Yixuan Li, and Rayadurgam Srikant. Enhancing the reliability of out-of-distribution image detection in neural networks. In *International Conf. on Learning Representations*, 2018. 1, 2
- [19] Weitang Liu, Xiaoyn Wang, John Owens, and Yixuan Li. Energy-based out-of-distribution detection. In *Advances in Neural Information Processing Systems*, 2020. 1, 2
- [20] Xixi Liu, Yaroslava Lochman, and Christopher Zach. Gen: Pushing the limits of softmax-based out-of-distribution detection. In *IEEE/CVF Conference on Computer Vision and Pattern Recognition*, 2023. 2
- [21] Ilya Loshchilov and Frank Hutter. Sgdr: Stochastic gradient descent with warm restarts. In *International Conf. on Learning Representations*, 2017. 6
- [22] Haodong Lu, Dong Gong, Shuo Wang, Jason Xue, Lina Yao, and Kristen Moore. Learning with mixture of prototypes for out-of-distribution detection. In *International Conf. on Learning Representations*, 2024. 1, 3, 9
- [23] Leland McInnes, John Healy, Nathaniel Saul, and Lukas Großberger. Umap: Uniform manifold approximation and projection. *The Journal of Open Source Software*, 3(29):861, 2018. 7
- [24] Quinn McNemar. Note on the sampling error of the difference between correlated proportions or percentages. *Psychometrika*, 1947. 6
- [25] Yifei Ming, Yiyu Sun, Ousmane Dia, and Yixuan Li. How to exploit hyperspherical embeddings for out-of-distribution detection? In *International Conf. on Learning Representations*, 2023. 1, 3, 8
- [26] Yuval Netzer, Tao Wang, Adam Coates, Alessandro Bisaccho, Baolin Wu, Andrew Y Ng, et al. Reading digits in natural images with unsupervised feature learning. In *Advances in Neural Information Processing Systems*, 2011. 5
- [27] Kemal Oksuz, Baris Can Cam, Emre Akbas, and Sinan Kalkan. Rank & sort loss for object detection and instance segmentation. In *International Conference on Computer Vision*, 2021. 1, 2, 3, 5
- [28] Adam Paszke, Sam Gross, Francisco Massa, Adam Lerer, James Bradbury, Gregory Chanan, Trevor Killeen, Zeming Lin, Natalia Gimelshein, Luca Antiga, et al. Pytorch: An imperative style, high-performance deep learning library. In *Advances in Neural Information Processing Systems*, 2019. 5
- [29] Avinash Ravichandran, Rahul Bhotika, and Stefano Soatto. Few-shot learning with embedded class models and shot-free meta training. In *International Conference on Computer Vision*, 2019. 3
- [30] Florian Schroff, Dmitry Kalenichenko, and James Philbin. Facenet: A unified embedding for face recognition and clustering. In *IEEE/CVF Conference on Computer Vision and Pattern Recognition*, 2015. 1, 3, 4
- [31] Jake Snell, Kevin Swersky, and Richard Zemel. Prototypical networks for few-shot learning. In *Advances in Neural Information Processing Systems*, 2017. 1, 3
- [32] Yiyu Sun, Yifei Ming, Xiaojin Zhu, and Yixuan Li. Out-of-distribution detection with deep nearest neighbors. In *International Conf. on Machine Learning*, 2022. 1, 2, 3, 4, 8
- [33] Jihoon Tack, Sangwoo Mo, Jongheon Jeong, and Jinwoo Shin. Csi: Novelty detection via contrastive learning on distributionally shifted instances. In *Advances in Neural Information Processing Systems*, 2020. 1
- [34] Laurens Van der Maaten and Geoffrey Hinton. Visualizing data using t-sne. *Journal of Machine Learning Research*, 9 (86):2579–2605, 2008. 7
- [35] Wouter Van Gansbeke, Simon Vandenhende, Stamatios Georgoulis, Marc Proesmans, and Luc Van Gool. Scan: Learning to classify images without labels. In *European Conference on Computer Vision*, 2020. 4, 5
- [36] Grant Van Horn, Oisín Mac Aodha, Yang Song, Yin Cui, Chen Sun, Alex Shepard, Hartwig Adam, Pietro Perona, and Serge Belongie. The inaturalist species classification and detection dataset. In *IEEE/CVF Conference on Computer Vision and Pattern Recognition*, 2018. 5
- [37] Sagar Vaze, Kai Han, Andrea Vedaldi, and Andrew Zisserman. Open-set recognition: A good closed-set classifier is

- all you need? In *International Conf. on Learning Representations*, 2022. 5
- [38] Haoqi Wang, Zhizhong Li, Litong Feng, and Wayne Zhang. Vim: Out-of-distribution with virtual-logit matching. In *IEEE/CVF Conference on Computer Vision and Pattern Recognition*, 2022. 5
- [39] Bernard L. Welch. The generalization of “student’s” problem when several different population variances are involved. *Biometrika*, 1947. 6
- [40] Hong-Ming Yang, Xu-Yao Zhang, Fei Yin, and Cheng-Lin Liu. Robust classification with convolutional prototype learning. In *IEEE/CVF Conference on Computer Vision and Pattern Recognition*, 2018. 4
- [41] Jingkang Yang, Pengyun Wang, Dejian Zou, Zitang Zhou, Kunyuan Ding, Wenxuan Peng, Haoqi Wang, Guangyao Chen, Bo Li, Yiyun Sun, et al. Openood: Benchmarking generalized out-of-distribution detection. In *Advances in Neural Information Processing Systems*, 2022. 2, 3
- [42] Jingkang Yang, Kaiyang Zhou, Yixuan Li, and Ziwei Liu. Generalized out-of-distribution detection: A survey. In *International Journal of Computer Vision*, 2024. 1
- [43] Jingyang Zhang, Jingkang Yang, Pengyun Wang, Haoqi Wang, Yueqian Lin, Haoran Zhang, Yiyun Sun, Xuefeng Du, Yixuan Li, Ziwei Liu, et al. Openood v1.5: Enhanced benchmark for out-of-distribution detection. *Journal of Data-centric Machine Learning Research*, 2024. 2, 3, 5
- [44] Bolei Zhou, Agata Lapedriza, Aditya Khosla, Aude Oliva, and Antonio Torralba. Places: A 10 million image database for scene recognition. In *IEEE Transactions on Pattern Analysis and Machine Intelligence*, 2017. 5
- [45] Fei Zhou, Peng Wang, Lei Zhang, Wei Wei, and Yanning Zhang. Revisiting prototypical network for cross domain few-shot learning. In *IEEE/CVF Conference on Computer Vision and Pattern Recognition*, 2023. 3

A. Selected Hyperparameters and OOD Post-Processing

For each in-distribution dataset and training objective, we select model hyperparameters based on validation ID classification accuracy under the OpenOOD protocol. When multiple OOD scoring rules are considered, we choose the rule with the better validation AUROC. The tuned hyperparameters are: learning rate (**LR**); embedding dimension (**ED**), used only for embedding-based objectives; and, for Prototype Loss, the center-loss weight (λ) and the temperature parameter (τ) used to convert distances to class probabilities.

For OOD scoring, we consider maximum softmax probability (**MSP**) and predictive entropy (**Entropy**) for Cross-Entropy and Prototype objectives, and we report results using the selected rule listed in Tables 1-3. For Triplet Loss, we use the standard nearest-neighbor distance in the learned embedding space (minimum distance to training embeddings) as the OOD score. For Average Precision (AP) Loss, we compute class probabilities via softmax and use entropy-based scoring.

For Triplet Loss optimization, we use different mining strategies depending on dataset complexity: random negative triplet mining for CIFAR-10, and semi-hard negative triplet mining for CIFAR-100 and ImageNet-200 (as defined in Section 3.2.2).

Objective	LR	ED	λ / τ	Triplet Mining	OOD score
AP Loss	0.08	–	– / –	–	Entropy
Cross-Entropy Loss	0.10	–	– / –	–	Entropy
Prototype Loss	0.10	64	0.01 / 0.1	–	Entropy
Triplet Loss	0.005	32	– / –	Random	1-NN distance

Table 1. Selected hyperparameters and OOD post-processing for CIFAR-10.

Objective	LR	ED	λ / τ	Triplet Mining	OOD score
AP Loss	0.08	–	– / –	–	Entropy
Cross-Entropy Loss	0.08	–	– / –	–	Entropy
Prototype Loss	0.10	128	0.001 / 0.1	–	MSP
Triplet Loss	0.0004	256	– / –	Semi-hard	1-NN distance

Table 2. Selected hyperparameters and OOD post-processing for CIFAR-100.

Objective	LR	ED	λ / τ	Triplet Mining	OOD score
AP Loss	0.10	–	– / –	–	Entropy
Cross-Entropy Loss	0.08	–	– / –	–	Entropy
Prototype Loss	0.10	128	0.001 / 0.1	–	MSP
Triplet Loss	0.0009	512	– / –	Semi-hard	1-NN distance

Table 3. Selected hyperparameters and OOD post-processing for ImageNet-200.

B. Extended Quantitative Results

In this section, we report extended results (mean \pm standard deviation) for each training objective across five independent runs on the CIFAR-10, CIFAR-100, and ImageNet-200 OpenOOD benchmarks (Tables 4-6). The best performance in each column is shown in **bold**, while the second-best is underlined. The corresponding selected hyperparameters and OOD post-processing rules for these runs are provided in Appendix A (Tables 1-3).

Loss Function	ID Accuracy (%)	Near-OOD AUROC (%)	Far-OOD AUROC (%)
AP Loss	94.93±0.20	88.80±0.19	92.34±0.53
Cross-Entropy Loss	94.95±0.25	88.23±0.42	90.98±0.47
Prototype Loss	95.06±0.14	87.87±0.37	91.28±0.51
Triplet Loss	93.56±0.18	88.85±0.20	92.25±0.58

Table 4. Extended performance comparison on CIFAR-10 OpenOOD benchmark.

Loss Function	ID Accuracy (%)	Near-OOD AUROC (%)	Far-OOD AUROC (%)
AP Loss	77.21±0.46	79.32±0.27	77.68±1.15
Cross-Entropy Loss	77.10±0.28	80.94±0.24	80.46±0.75
Prototype Loss	78.18±0.54	79.95±0.33	79.85±1.42
Triplet Loss	69.00±0.30	76.95±0.27	80.50±1.05

Table 5. Extended performance comparison on CIFAR-100 OpenOOD benchmark.

Loss Function	ID Accuracy (%)	Near-OOD AUROC (%)	Far-OOD AUROC (%)
AP Loss	86.71±0.30	82.47±0.20	90.54±0.28
Cross-Entropy Loss	86.66±0.22	83.54±0.19	91.16±0.25
Prototype Loss	86.07±0.34	80.78±0.17	89.73±0.23
Triplet Loss	68.12±0.22	74.44±0.14	84.70±0.23

Table 6. Extended performance comparison on ImageNet-200 OpenOOD benchmark.

C. Extended Qualitative Analysis

C.1. ID vs OOD Comparison

To complement the quantitative results, we analyze the embedding geometry induced by different training objectives using t-SNE and UMAP projections.

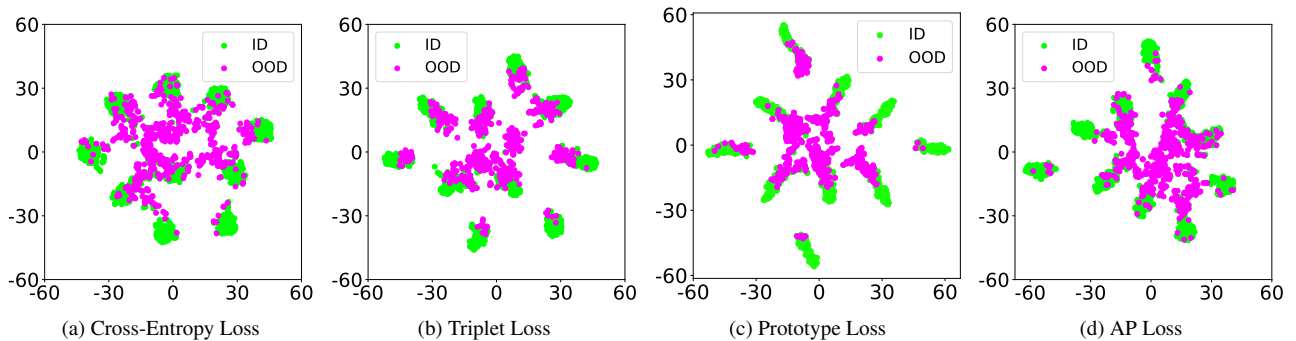


Figure 5. t-SNE Visualizations for ID vs OOD Comparison

Figure 5 illustrates the distribution of the ID and OOD data points produced by the models trained with different loss functions. The figures are generated using the t-SNE method and the points are colored to separate the ID and OOD samples.

In the two-dimensional projections, the in-distribution classes appear as relatively compact clusters, with samples visually grouped together and separated from other clusters. While dimensionality reduction methods do not preserve exact geometric relationships, this qualitative pattern is broadly consistent with the high ID accuracy observed on CIFAR-10 (all methods exceeding 93%), suggesting that the learned representations remain discriminative for in-distribution classification.

In the projections, the ID clusters appear relatively evenly distributed across the two-dimensional space, which makes it difficult to infer detailed semantic relationships between classes from the visualization alone.

In the projected embedding space, many OOD samples appear separated from the main ID clusters, reflecting their distributional difference from the training data. However, some OOD instances lie close to specific ID clusters, indicating that some OOD datasets contain samples with visual features similar to those of the in-distribution classes, which can make detection more difficult.

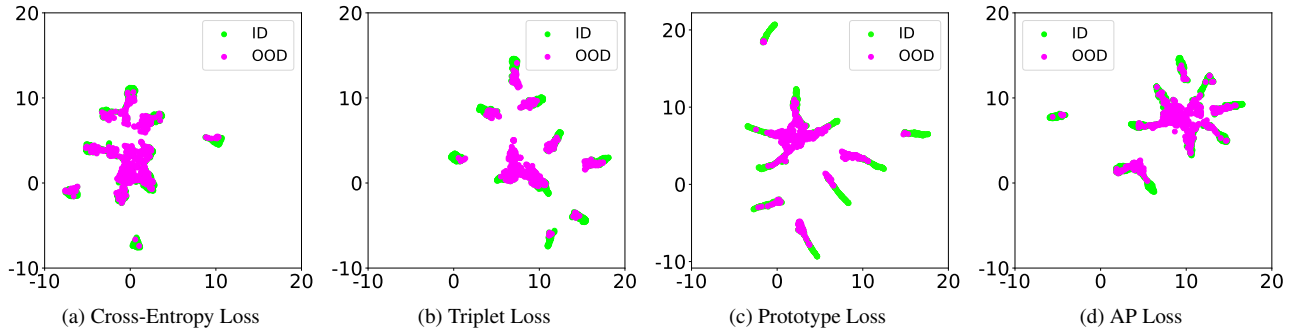


Figure 6. UMAP Visualizations for ID vs OOD Comparison

Figure 6 shows the visualizations of the embeddings generated by the UMAP method, which is often used to provide a complementary view of both local and broader structural patterns in the data.

In comparison to the t-SNE results, where the ID clusters are distributed relatively homogeneously, the UMAP visualizations provide additional insight into the relative arrangement of ID clusters in the two-dimensional space, offering qualitative cues about potential semantic relationships between classes in CIFAR-10.

Similar to the t-SNE projections, many OOD samples appear positioned away from the dense ID clusters and are not strongly aligned with any single ID class. However, the presence of OOD data points close to the ID clusters is more pronounced in the UMAP visualizations, suggesting that detecting some OOD samples may be challenging, as their embeddings are similar to those of the ID samples.

C.2. ID vs Near-OOD and Far-OOD Comparison

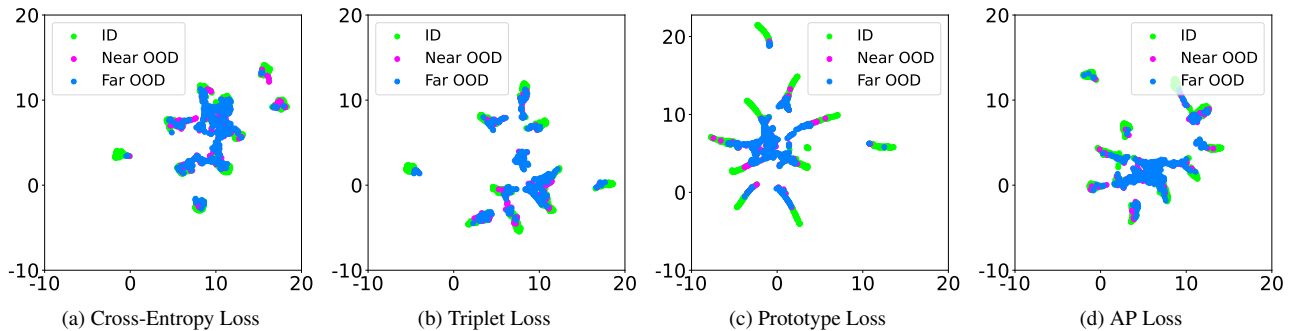


Figure 7. UMAP Visualizations for ID vs Near-OOD and Far-OOD Comparison

Figure 7 shows UMAP embeddings for in-distribution (ID), near-OOD, and far-OOD samples. In the projections, far-OOD samples tend to appear more separated from the main ID clusters, whereas near-OOD samples often appear closer to certain ID clusters. These patterns support our detection strategies and complement our quantitative findings.